Molecular Cell
Article

Heterohexameric Ring Arrangement of the Eukaryotic Proteasomal ATPases: Implications for Proteasome Structure and Assembly

Robert J. Tomko, Jr.,[1] Minoru Funakoshi,[1,2] Kyle Schneider,[1] Jimin Wang,[1] and Mark Hochstrasser[1,*]
[1]Department of Molecular Biophysics and Biochemistry, Yale University, 266 Whitney Avenue, New Haven, CT 06520-8114, USA
[2]Present address: Graduate School of Natural Science and Technology, Okayama University, Tsushima-naka 2-1-1, Kita-ku, Okayama 700-8530, Japan
*Correspondence: mark.hochstrasser@yale.edu
DOI 10.1016/j.molcel.2010.02.035

SUMMARY

The proteasome has a paramount role in eukaryotic cell regulation. It consists of a proteolytic core particle (CP) bound to one or two regulatory particles (RPs). Each RP is believed to include six different AAA+ ATPases in a heterohexameric ring that binds the CP while unfolding and translocating substrates into the core. No atomic-resolution RP structures are available. Guided by crystal structures of related homohexameric prokaryotic ATPases, we use disulfide engineering to show that the eukaryotic ATPases form a ring with the arrangement Rpt1-Rpt2-Rpt6-Rpt3-Rpt4-Rpt5 in fully assembled proteasomes. The arrangement is consistent with known assembly intermediates. This quaternary organization clarifies the functional overlap of specific RP assembly chaperones and led us to identify a potential RP assembly intermediate that includes four ATPases (Rpt6-Rpt3-Rpt4-Rpt5) and their cognate chaperones (Rpn14, Nas6, and Nas2). Finally, the ATPase ring structure casts light on alternative RP structural models and the mechanism of RP action.

INTRODUCTION

The highly conserved ubiquitin-proteasome system is responsible for a large fraction of the regulatory and quality control protein degradation that takes place in eukaryotic cells (Ravid and Hochstrasser, 2008; Finley, 2009). Most substrates are first modified by polyubiquitin chains, which then target the substrates to the 26S proteasome for degradation. Proteasomes are readily split into a 20S proteasome core particle (CP) and a 19S regulatory particle (RP). The CP has a cylindrical structure with a central chamber in which the protease active sites are located. The RP binds in an ATP-dependent fashion to one or both ends of the CP, controlling access to the narrow pores at the ends of the CP cylinder.

The RP can be separated under certain conditions into subcomplexes called the lid and the base (Marques et al., 2009; Finley, 2009). The base includes six paralogous AAA+ ATPases and three non-ATPase subunits (Rpn1, Rpn2, and Rpn13). The full RP has at least 19 different subunits. Protein substrate binding, unfolding, and translocation into the CP are major functions of the RP base. The primary biochemical activity attributed to the lid is the cleavage of polyubiquitin chains from substrates prior to or during their degradation.

Crystal structures have been reported for the CP from archaea, actinobacteria, and several eukaryotes (Marques et al., 2009). In contrast, atomic-resolution structures are unavailable for the full 26S proteasome, the RP, or any of the RP subcomplexes, although electron microscopy (EM) continues to yield important global structural information about the proteasome (da Fonseca and Morris, 2008; Nickell et al., 2009). EM and biochemical analyses indicate that the RP is conformationally heterogeneous and may vary in composition, making crystallographic approaches challenging.

This dearth of high-resolution structural information has led to a number of uncertainties and controversies regarding both the structure of the RP and its assembly. By analogy to other AAA+ ATPases, it is thought that the six proteasomal ATPases of the eukaryotic RP form a hexameric ring, which binds the surface of the CP cylinder (Marques et al., 2009). Symmetry analysis of reconstructions from single-particle EM images of the proteasome is consistent with this proposal (Forster et al., 2009). Assignment of individual ATPases to the 6-fold symmetric density distribution was modeled but has not been verified experimentally. Thus, it has not yet been formally demonstrated that the Rpts form a ring as part of the RP, let alone a uniquely ordered heterohexameric one. Exactly how the base associates with the lid and where the non-ATPase subunits are located represent additional uncertainties. For example, recent EM and atomic force microscopy studies have suggested that the two largest RP subunits, Rpn1 and Rpn2, fold into toroids that stack on one another over the pore of the CP cylinder (Rosenzweig et al., 2008; Effantin et al., 2009). In a model that integrates these subunits into the remainder of the RP, the axially aligned Rpn1 and Rpn2 toroids are surrounded by a ring of ATPase subunits and protrude distally toward the lid (Rosenzweig et al., 2008). In contrast, other EM reconstructions have suggested a more peripheral placement of the large Rpn1 and/or Rpn2 subunits, although the positions of these subunits were not directly examined (da Fonseca and Morris, 2008; Nickell et al., 2009).

Recent studies of RP assembly have accentuated the need for unambiguous data on RP subunit arrangement (Le Tallec et al., 2009; Funakoshi et al., 2009; Saeki et al., 2009; Kaneko et al., 2009; Park et al., 2009; Thompson et al., 2009; Hendil et al., 2009). At least four assembly chaperones facilitate the assembly of the RP base (reviewed in Besche et al., 2009). Each of these factors associates with specific base ATPase subunits as part of assembly intermediates. For example, the yeast assembly factor Nas6 (called gankyrin in humans) binds to the Rpt3 ATPase, and the Rpn14 chaperone (human PAAF1) binds to Rpt6. Genetic analysis in yeast revealed a close overlap in the function of Nas6 and Rpn14, which would suggest that the ATPases to which they bind, Rpt3 and Rpt6, are in close proximity (Funakoshi et al., 2009; Saeki et al., 2009). On the other hand, earlier models for ATPase subunit arrangement had these subunits on opposing sides of the ring (Hartmann-Petersen et al., 2001; Fu et al., 2001). Some protein-protein interaction data do suggest that Rpt3 and Rpt6 can associate more intimately, but other results argue against this (summarized in Fu et al., 2001). These discrepancies may reflect RP heterogeneity, differences in assay methods, or the fact that interactions in fully assembled proteasomes were not usually distinguished from those in assembly intermediates or nonnative complexes. The remaining base assembly chaperones are part of intermediates or modules containing two ATPases each: Nas2 (p27 in humans) associates with Rpt4 and Rpt5, while Hsm3 (human S5b) interacts with Rpt1-Rpt2 (and the non-ATPase Rpn1). Here again, Nas2 and Hsm3 have been found to have partially redundant functions, yet the ATPases to which they bind are not contiguous in some models of the ATPase ring.

A definitive determination of the quaternary organization of the eukaryotic proteasomal ATPases would clear up many of these uncertainties regarding RP assembly and structure. The recent publication of several crystal structures of simpler homohexameric AAA+ ATPase complexes from archaeal and actinobacterial species (Zhang et al., 2009; Djuranovic et al., 2009) now makes possible structure-guided methods to do this. These ATPases, called proteasome-activating nucleotidase (PAN) in archaea and ATPase-forming ring-shaped complex (ARC) in actinobacteria, are orthologous to the eukaryotic Rpt subunits. Full-length proteins could not be crystallized, but a hexamer of an N-terminal element was isolated and described structurally. In one study, a C-terminal segment encompassing the AAA+ domain and C-terminal helical domain was also crystallized, albeit as a monomer (Zhang et al., 2009). The N-terminal segment consists of a coiled coil (CC)-forming helix followed by one or two oligonucleotide/oligosaccharide-binding (OB) domains. The crystal structure of PAN reveals a trimer of dimers with each dimer made of so-called *cis* and *trans* subunits, as defined by the peptide-bond configuration of a critical proline between the CC and OB domains (Pro91 for the *M. jannaschii* protein; Figure 1B). Proline is unusual in its ability to form a *cis* peptide-bond configuration with the preceding residue in a polypeptide. The six OB domains from the six subunits have pseudo-6-fold symmetry, while the CCs show only 3-fold symmetry. The OB domains of the hexamer encircle a narrow pore of ~11–13 Å, and residues in the interfaces between the OB domains can be aligned with eukaryotic sequences in these regions despite relatively weak sequence conservation.

We used such sequence alignments to pick pairs of residues in different yeast Rpt subunits to replace with cysteine. The hope was that these would be able to form disulfide bonds under oxidizing conditions if the two cysteines were juxtaposed in neighboring subunits. Using this structure-guided disulfide-engineering strategy, we were able to define a uniquely ordered heterohexameric arrangement of ATPases in the proteasomal RP. The approach is general and can be used in other systems where simpler multisubunit structures from archaea or bacteria are known. The different eukaryotic ATPase OB domain interactions are structurally similar to the homomeric subunit interactions in PAN and ARC. This allowed us to infer that the eukaryotic ATPases also form a very narrow central channel that cannot accommodate other RP subunits, in particular the large Rpn1 and Rpn2 base subunits, without massive rearrangement. The experimentally determined organization juxtaposes those ATPase subunits in the ring that are bound by functionally redundant assembly factors, thereby providing a structural rationalization for the close functional overlap of these pairs of chaperones. It also led us to find evidence for a potential assembly intermediate containing four of the six ATPase subunits and three of the four RP base assembly chaperones.

RESULTS

Strategy for Determining ATPase Arrangement in the Eukaryotic RP

The six different ATPases in the eukaryotic proteasome are assumed to assemble into a uniquely ordered ring. In principle, such a ring could have any of 120 different arrangements containing six different subunits; if individual subunits could be present more than once per ring, a far greater number of arrangements would be possible. While existing biochemical data place constraints on possible arrangements, not all the results are in agreement. A potentially simplifying assumption derives from the sequence similarity of the eukaryotic proteasomal ATPases to prokaryotic PAN and ARC ATPases, which form hexameric rings from six identical subunits: analogous to the PAN/ARC rings, the eukaryotic Rpt subunits might form a hexameric ring from a trimer of "*cis-trans*" heterodimers (models 3 and 4 in Figure 1A). The eukaryotic *cis* subunits are predicted by the presence of a conserved proline residue corresponding to Pro91 in PAN (Zhang et al., 2009; Djuranovic et al., 2009).

As noted, the yeast Rpt1 and Rpt2 subunits are part of an RP base assembly intermediate, and Rpt4 and Rpt5 are part of another. These pairs of ATPases could potentially follow the *cis-trans* subunit pairing suggested by alignment with the PAN/ARC sequences. This leaves Rpt3 and Rpt6. Rpt3 has a proline at the position aligning with the absolutely conserved PAN/ARC proline, whereas Rpt6 does not, which would be consistent with their forming a *cis-trans* pair. Recent biochemical data with mammalian cells suggest that these two ATPases are part of assembly intermediates that lack the other ATPases (Kaneko et al., 2009; Hendil et al., 2009; Thompson et al., 2009). However, other results for eukaryotic ATPase subunit arrangement place Rpt3 and Rpt6 on opposite sides of the ring; this arrangement is based on chemical crosslinking and other protein-protein interaction data (model 1, Figure 1A) (Hartmann-Petersen et al.,

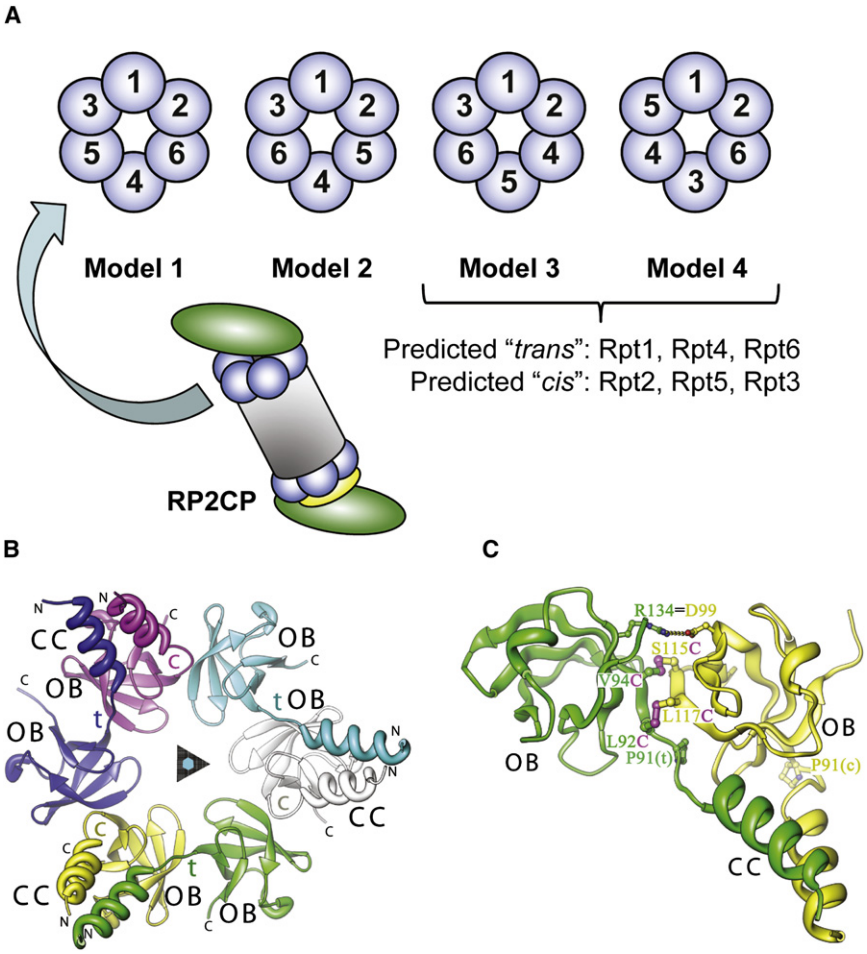

Figure 1. Potential Arrangements of Eukaryotic Proteasomal ATPase Subunits

(A) The six ATPase subunits (Rpt1–Rpt6) of the 26S proteasome and four possible ways of arranging them (out of 120) into a heterohexameric ring. Model 1 had been proposed based on chemical crosslinking and other data (Fu et al., 2001); model 2 was suggested recently by Kaneko et al. (2009); and models 3 and 4 are the two possible arrangements of putative "*cis-trans*" heterodimers Rpt1-2, Rpt4-5, and Rpt6-3 if *cis* and *trans* subunits alternate around the ring, as they do in the prokaryotic PAN and ARC rings.

(B) The trimer-of-dimers structure of the homohexameric *M. jannaschii* PAN subcomplex I (PDB 3H43) imposed by coiled-coil (CC) formation between *cis* (c) and *trans* (t) subunits.

(C) Interface between archaeal PAN OB domains of neighboring subunits in a *cis-trans* dimer. Side chains are shown for interacting residues that were used for testing paralogous Rpt OB domain interactions in yeast. Disulfide bonds (magenta) are modeled for pairs of residues whose putative yeast counterparts were substituted with cysteines. Also indicated are Pro91, which alternates between *cis* and *trans* configurations in neighboring subunits, and the prominent Arg134-Asp99 intersubunit pairing.

2001; Fu et al., 2001). It is therefore possible that Rpt neighbors rearrange during the assembly process or that the model placing Rpt3 and Rpt6 on opposite sides of the ring is incorrect (or both).

In earlier work, we were able to determine nearest-neighbor positions of eukaryotic CP subunits by reference to crystallographic data from the much simpler archaeal CP and use of structure-guided pseudoreversion analysis (Chen and Hochstrasser, 1996; Arendt and Hochstrasser, 1997). These analyses were based on the premise that single mutations in predicted interfacial residues for a pair of neighboring subunits will often be deleterious, but that simultaneous compensatory mutations would suppress the single mutant defects. Our attempts at pseudoreversion analysis with the Rpt6-Rpt3 equivalents of *M. jannaschii* PAN Arg134 and Asp99 (Figure 1C) were unsuccessful, as no growth defects could be detected for the single *rpt6-R116E* or *rpt3-E101R* mutants (data not shown).

Another approach to protein-protein interaction mapping, which we have also used in our CP studies, is to replace residues predicted to interact across a subunit interface with cysteines and then crosslink the two subunits in vitro by inducing disulfide bond formation (Velichutina et al., 2004; Kusmierczyk et al., 2008). We attempted to use such disulfide engineering to test the putative Rpt3-Rpt6 association. A survey of the *cis-trans* subunit interface of archaeal PAN suggested several residues which, if replaced by cysteines, might form intersubunit disulfide bonds (Figure 1C). We focused on two of these pairs in the OB domain because their sequences were not highly conserved, so mutating them would be unlikely to interfere with ATPase function. Attempts at disulfide engineering of the Rpt6-Rpt3 equivalents of *M. jannaschii* PAN Leu92 and Leu117 failed (data not shown), but experiments aimed at the Rpt6 and Rpt3 equivalents of PAN Val94 (*trans*) and Ser115 (*cis*) were more successful.

Rpt3 and Rpt6 Are Direct Neighbors in the 26S Proteasome

Mutations were introduced into plasmid-borne alleles of *RPT3* and *RPT6* to create the desired cysteine substitutions. The mutated plasmids were transformed into yeast strain MHY5658, which has chromosomal deletions of both *RPT3* and *RPT6* but carries the two wild-type alleles on a *URA3* plasmid. Following transformation with the mutated plasmids, yeast cells that had lost the original *URA3* plasmid were selected. Disulfide crosslinking between Rpt6-S70C and Rpt3-V119C was induced by incubation of cell lysates with the oxidant $CuCl_2$ (Velichutina et al., 2004). Anti-Rpt3 immunoblotting of proteins separated by nonreducing SDS-polyacrylamide gel electrophoresis (SDS-PAGE) revealed a time-dependent loss of the Rpt3 monomer along with the appearance of a prominent higher molecular mass species (Figure 2A). This larger species was only seen if both Rpt subunits contained the appropriately engineered Cys residue and were sensitive to reducing agents;

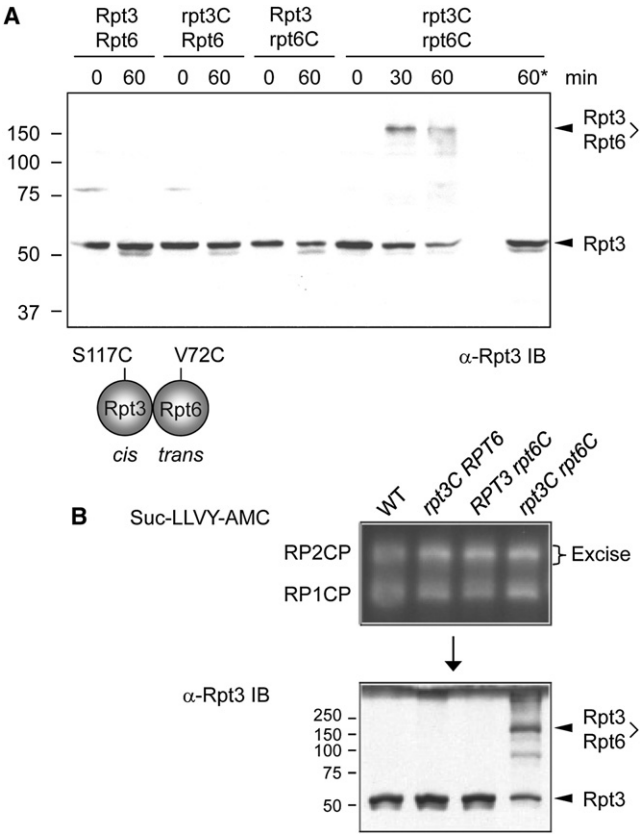

Figure 2. Rpt3 and Rpt6 Are Direct Neighbors in the Yeast 26S Proteasome

(A) Disulfide crosslinking of Rpt3 and Rpt6 subunits with the indicated Cys substitutions. Crosslinking was induced in whole-cell lysates (WCL) with $CuCl_2$ for the indicated times. Proteins were resolved by nonreducing SDS-PAGE and examined by anti-Rpt3 immunoblotting. For the last lane (60*), the WCL was incubated for 10 min in DTT prior to gel loading.

(B) Rpt3 and Rpt6 associate in doubly capped proteasomes (RP2CP). Proteasomes were resolved by nondenaturing PAGE, crosslinked, and visualized by overlaying with a fluorogenic peptide substrate (top). A gel strip containing the RP2CP species was excised and placed atop a nonreducing SDS gel, and the samples were analyzed by anti-Rpt3 immunoblotting (bottom).

when dithiothreitol (DTT) was added to the sample prior to electrophoresis, the crosslinked species was eliminated (Figure 2A, last lane).

The Rpt3-Rpt6 species migrated more slowly than its predicted mass of ~93 kD. Similarly anomalous migration was observed previously with crosslinked CP subunits (Kusmierczyk et al., 2008) and is likely due to the branched structure of the disulfide-linked proteins. Additional DTT-sensitive species of lower abundance were also seen in these experiments (Figure 2A). Again, a similar phenomenon was observed with disulfide engineering of CP subunits (Kusmierczyk et al., 2008). These extra bands may reflect the presence of four native Cys residues in Rpt6, which might crosslink to one another or form other oxidized products that change the mobility of the complex. This would be consistent with the drop in the major Rpt3-Rpt6 band after longer times of oxidation when these other species become more prominent (Figure 2A).

The crosslinking results strongly support the hypothesis that Rpt3 and Rpt6 are direct neighbors in the RP base; however, these experiments were done with whole-cell extracts, so the crosslinks between Rpt3 and Rpt6 might have occurred only in proteasome assembly intermediates or even dead-end RP subcomplexes. Similar caveats apply to much of the published pairwise RP subunit interaction data, such as chemical crosslinking or yeast two-hybrid analysis. To address this problem, we first isolated doubly capped 26S proteasomes (RP2CP) and then subjected them to crosslinking (Kusmierczyk et al., 2008). Yeast cell extracts were fractionated by native PAGE, and after crosslinking the excised RP2CP species were analyzed by nonreducing SDS-PAGE and immunoblotting (Figure 2B, bottom). As was seen with whole-cell lysates, the disulfide-linked Rpt3-Rpt6 species was readily formed in fully assembled 26S proteasomes. Because disulfide bond formation requires that the two cysteine side chains be within a few angstroms of one another, we can conclude with high confidence that the interaction seen occurs between neighboring subunits in the ring.

These data indicate first that the OB domains of different eukaryotic proteasomal ATPases can interact in a way very similar to the rigid OB domain associations in prokaryotic PAN/ARC homohexameric ring complexes, and second that Rpt3 and Rpt6 are direct neighbors in the 26S proteasome.

Rpt5-Rpt4 and Rpt2-Rpt1 Are Also "*cis-trans*" Heterodimer Pairs

Extrapolating from the Rpt3-Rpt6 crosslinking results, similar binding interactions should occur at all the Rpt-Rpt interfaces. Hence, it should be possible to use the positions equivalent to Rpt3-Val119 and Rpt6-Ser70 in other Rpt subunits for cysteine substitution and protein-protein interaction mapping by disulfide engineering. Since biochemical data link Rpt5 and Rpt4 (Funakoshi et al., 2009; Saeki et al., 2009), we hypothesized that these subunits would form a second *cis-trans* dimer within the ATPase ring. Rpt5-Thr126 and Rpt4-Ile105 were mutated to Cys residues and tested for disulfide formation by the same methods used for Rpt3-Rpt6 crosslinking. A specific disulfide between Rpt5-T126C and Rpt4-I105C was induced in yeast lysates as visualized by either anti-Rpt4 (Figure 3A) or anti-Rpt5 (Figure 3B) immunoblotting. Crosslinking was only observed if both subunits contained the engineered Cys residue, and the linkage could be eliminated by DTT treatment (data not shown). Finally, the two ATPases could also be crosslinked in intact 26S proteasomes (Figure S1). These results lead us to conclude that Rpt5 and Rpt4 are *cis-trans* neighbors in the yeast RP.

Analogous experiments were performed for the remaining suspected *cis-trans* pair, Rpt2-Rpt1. The sequence alignments between Rpt1 and the PAN/ARC ATPases differed in the two studies describing the prokaryotic structures (Zhang et al., 2009; Djuranovic et al., 2009); our sequence analysis matched the alignment of Djuranovic et al. (2009). When both Rpt2-Asp127 and Rpt1-Val99 were mutated to Cys residues, a disulfide bond could be induced between the two subunits either in whole-cell lysates (Figure 4A) or in isolated 26S proteasomes (Figure 4B). The crosslink was also sensitive to reducing agent (data not shown). Importantly, the "*trans-cis*" association between Rpt1 and Rpt2 was unique. Tests for disulfide formation

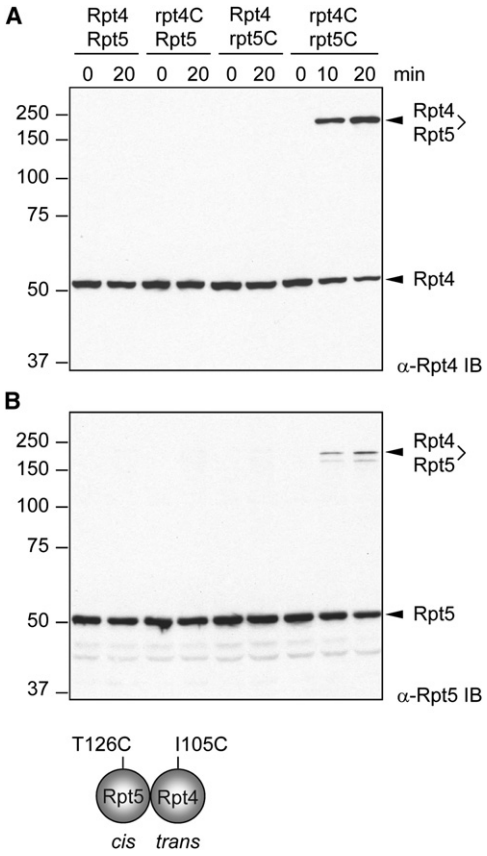

Figure 3. Rpt4 and Rpt5 OB Domains Associate as Predicted by the "*cis-trans* Dimer" Model

(A) Disulfide crosslinking of Rpt4 and Rpt5 subunits with the Cys substitutions shown at bottom of figure. Crosslinking was induced in WCL and analyzed as in Figure 2A (anti-Rpt4 immunoblot).

(B) Aliquots from the same samples used for (A) but evaluated by anti-Rpt5 blotting.

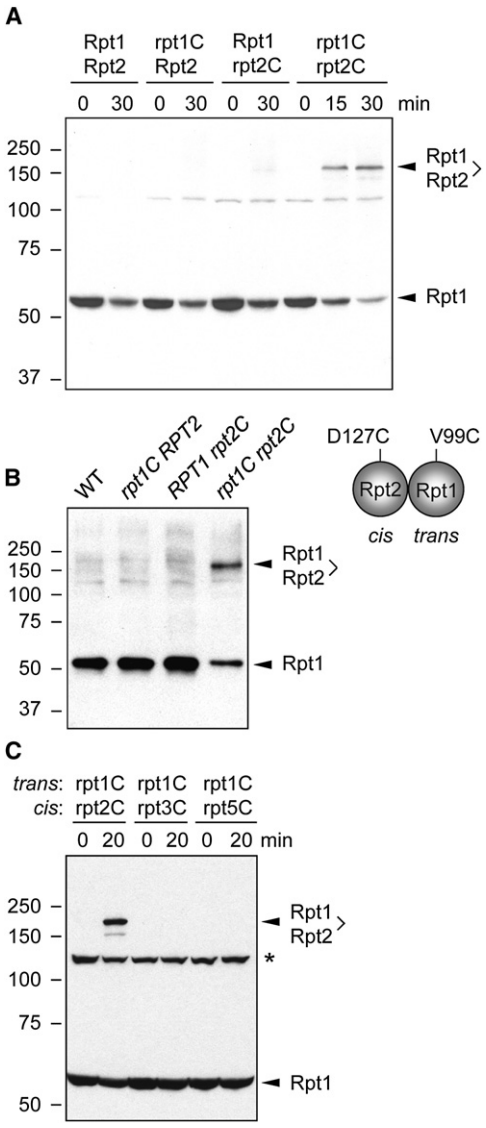

Figure 4. Rpt1 Pairs Specifically with Rpt2

(A) Disulfide crosslinking of Rpt1 and Rpt2 subunits with the Cys substitutions indicated in the cartoon. Crosslinking was induced in WCL and analyzed as in Figure 2A (anti-Rpt1 immunoblot).

(B) Rpt1 and Rpt2 associate in mature (RP2CP) proteasomes. Analysis was as in Figure 2B but with anti-Rpt1 immunoblotting.

(C) Comparison of Rpt1-V99C ("*trans*" subunit) crosslinking to the three predicted "*cis*" subunits with cysteine substitutions at aligned positions: Rpt2-D127C, Rpt3-S117C, and Rpt5-T126C. Crosslinking was induced in WCL and analyzed as in (A). Asterisk, unknown yeast protein recognized by anti-Rpt1 antibody.

between Rpt1-V99C (*trans*) and engineered forms of the two other *cis* subunits, Rpt3-S117C and Rpt5-T126C (see Figures 2 and 3) failed to reveal any crosslinking, in contrast to Rpt2-D127C (Figure 4C).

In summary, the data indicate that the six different proteasomal ATPases in the eukaryotic proteasome form three specific pairs: Rpt1-Rpt2, Rpt4-Rpt5, and Rpt6-Rpt3. These pairings are consistent with most, but not all, previous biochemical data and are in concordance with the trimer-of-dimers arrangement of the PAN/ARC homohexameric ATPase rings. The data rule out two previously proposed models for ATPase arrangement (models 1 and 2 in Figure 1A).

Placement of the Three *cis-trans* Dimers into a Heterohexameric Ring

In the PAN and ARC rings, the *cis-trans* homodimers are positioned such that *cis* and *trans* subunits alternate around the ring. If *cis* and *trans* subunits of the eukaryotic heterohexamer alternate in this fashion as well, then there are only two ways in which the three Rpt heterodimers can be placed within the ring (Figure 1A, models 3 and 4). To distinguish between these two possibilities, we tested whether Rpt1 (a *trans* subunit that pairs with the Rpt2 *cis* subunit) makes an interdimer contact with Rpt3 or Rpt5. The *cis-trans* dimer interface contacts made by the OB domain residues in the prokaryotic ATPase structures that were chosen for disulfide engineering in yeast are very similar to the contacts between neighboring dimers. We therefore

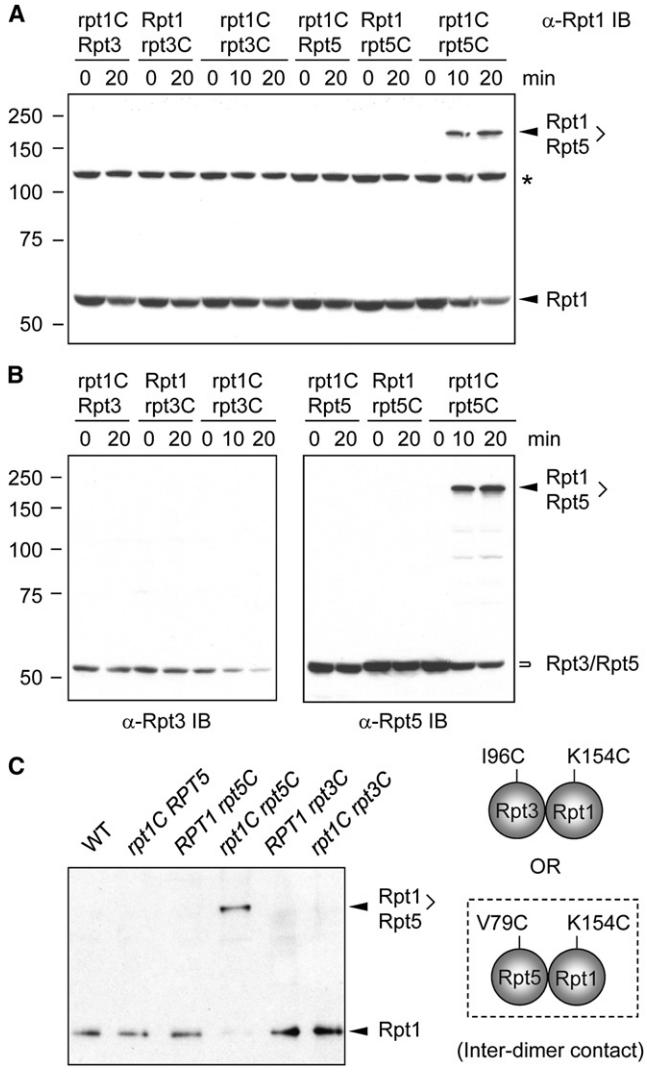

Figure 5. Analysis of Interdimer ATPase Interactions of the Yeast Proteasome

(A) Comparison of potential Rpt1-Rpt3 versus Rpt1-Rpt5 interdimer crosslinks in WCL by anti-Rpt1 immunoblotting.

(B) Same as in (A), except samples were tested by anti-Rpt3 and anti-Rpt5 immunoblotting.

(C) Rpt1 and Rpt5 associate in the intact RP2CP. Analysis was done as in Figure 4B. The residues mutated to cysteine are shown in the cartoon (the observed Rpt5-V79C–Rpt1-K154C disulfide is indicated by the dashed box).

compared the ability of Rpt1-K154C to form an engineered disulfide with Rpt3-I96C versus Rpt5-V79C (Figure 5). Based on anti-Rpt1 immunoblot analysis, a crosslink with the latter subunit could form readily, whereas no disulfide with Rpt3-I96C was detected (Figure 5A). This was confirmed by anti-Rpt5 and anti-Rpt3 immunoblotting (Figure 5B). The specific Rpt1-K154C–Rpt5-V79C crosslink was also observed in fully assembled RP2CP proteasomes (Figure 5C). These results indicate that Rpt1 associates with Rpt5 in the hexameric ring, consistent with model 4 and inconsistent with all the other models shown in Figure 1A.

We derived further support for this unique arrangement of ATPases by testing interdimer contacts between Rpt3 and Rpt4. A specific disulfide was formed between Rpt3-I96C and Rpt4-R126C based on both anti-Rpt3 and anti-Rpt4 immunoblotting (Figure S2). This also demonstrated that Rpt3-I96C, which had failed to crosslink to Rpt1-K154C (Figure 5), was competent for intersubunit crosslinking. As an additional control, we found that Rpt3-I96C could not be crosslinked to Rpt4-I128C (data not shown); the latter protein had a cysteine substitution at a position also predicted to be part of the Rpt3-Rpt4 interface but not near Rpt3-I96.

Considered together, these structure-guided disulfide engineering results (see Figure 7A) provide definitive evidence that the six different eukaryotic proteasomal ATPases form a uniquely ordered ring and interact through their OB domains in a manner highly similar to the archaeal PAN homohexameric subunit interactions.

Potential Assembly Intermediate Containing Four ATPases

The revised arrangement of the RP ATPases led us to reexamine the question of whether assembly modules bearing particular Rpt heterodimers combine to form specific higher-order complexes, which could represent intermediates in RP base assembly. Previously, we had found that the FLAG-tagged Hsm3 assembly factor (which is part of the Hsm3-Rpt1-Rpt2-Rpn1 assembly module—the "Hsm3 module") could coprecipitate base and RP complexes that also contained the Nas6 and Rpn14 chaperones; the Nas2 chaperone, in contrast, was not detected in these larger complexes (Funakoshi et al., 2009). On the other hand, Saeki et al. reported that about 4%–5% of precipitated FLAG-EGFP-tagged Nas2 was associated with the full RP (Saeki et al., 2009). The latter finding might reflect greater detection sensitivity or, alternatively, a low level of nonspecific binding between the RP and Nas2-fusion protein (consistent with the apparent failure of this tagged Nas2 to coprecipitate free base, unlike all the other chaperones). These authors also found that untagged Nas2 and Hsm3 were both efficiently coprecipitated by triply FLAG-tagged Nas6 or Rpn14, which would be consistent with all four chaperones being present in the same particle.

To help understand these differences, we compared the ability of different triply FLAG-tagged chaperones to coprecipitate untagged Nas2 in buffers with two different salt concentrations (Figure 6A). In agreement with Saeki et al. (2009), we found that tagged Nas6 or Rpn14 could coprecipitate Nas2 from whole-cell lysates under both conditions. In marked contrast, tagged Hsm3 did not bring down detectable amounts of Nas2. This was not an artifact of tagging Hsm3, because we also could not precipitate untagged Hsm3 with FLAG-tagged Nas2 (Figure 6B). Hence, these results imply that Nas2 and Hsm3 do not stably associate in the same complex. This seemed at odds with the aforementioned data, which had suggested that all four chaperones were present together in an RP precursor. The paradox would be resolved if the Nas2 precipitated with Nas6 or Rpn14 was not a constituent of full RP (or RP base) complexes, as had been assumed, but instead was in an intermediate that lacked the Hsm3 module.

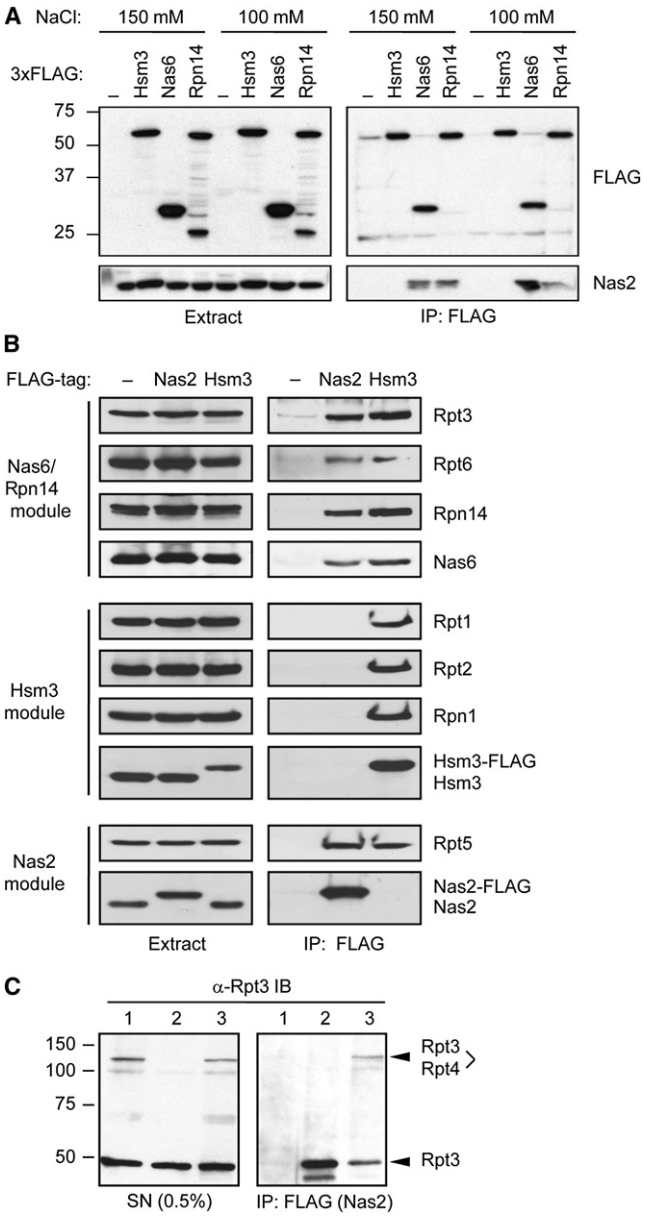

Figure 6. A Nas2-Bound RP Base Intermediate Lacking the Hsm3 Assembly Module

(A) Anti-FLAG immunoprecipitations from extracts of the indicated strains followed by immunoblot analysis with antibodies to Nas2 or FLAG. Extracts were made in buffer containing either 150 mM NaCl, as described by Funakoshi et al. (2009), or 100 mM NaCl, as in Saeki et al. (2009).

(B) Anti-Nas2-FLAG immunoprecipitates contain the Rpt4-Rpt5 and Rpt6-Rpt3 dimers (and associated assembly factors), but not components of the Hsm3 module. Only proteins known to be in the complex are depicted.

(C) The chaperone-bound two-module ATPase complex has Rpt3 and Rpt4 in their mature ring positions. Interdimer disulfide crosslinking was induced for 20 min in the anti-FLAG eluates (right panel) or supernates (SN). (The vast majority of crosslinked Rpt3-Rpt4 should be in mature RP, as seen from the SNs of the anti-FLAG purifications [lanes 1 and 3]. Strains used were (1) *rpt3-I96C rpt4-R126C NAS2*, (2) *RPT3 RPT4 NAS2-FLAG3*, and (3) *rpt3-I96C rpt4-R126C NAS2-FLAG3*.

We tested the hypothesis of an intermediate containing the Nas2-Rpt4-Rpt5 module ("Nas2 module") and the Nas6-Rpt3/Rpn14-Rpt6 module ("Nas6/Rpn14 module"), but not the Hsm3 module, by analyzing protein binding to Nas2 in vivo (Figure 6B). Strikingly, FLAG-tagged Nas2 coprecipitated all subunits of the Nas6/Rpn14 module (Rpt3, Rpt6, Nas6, and Rpn14) but none from the Hsm3 module (Rpn1, Rpt1, Rpt2, and Hsm3). As expected, Rpt5 was also coprecipitated. (In addition, epitope-tagged Rpn2 could coprecipitate Nas2, indicating that the two-module complex has at least one additional RP subunit [Figure S3].) Tagged Hsm3, in contrast, coprecipitated components of both the Nas6/Rpn14 and Nas2 modules (but not the Nas2 chaperone itself), presumably when Hsm3 is associated with the full RP or RP base precursors.

If the Nas2-bound two-module complex is on-pathway for RP base assembly, one would predict that the two ATPase heterodimers will be in the same relative positions as in the mature RP. To test this, we used a strain expressing Rpt3-I96C (Nas6/Rpn14 module) and Rpt4-R126C (Nas2 module) as well as triply FLAG-tagged Nas2 and determined if the two ATPases could be disulfide crosslinked in the anti-Nas2-FLAG eluate (Figure 6C). The diagnostic crosslinked species was indeed observed (right panel, lane 3). This result implies that this two-module intermediate is not an aberrant off-pathway assembly complex.

DISCUSSION

In this study, we have used structure-guided disulfide engineering to determine the quaternary arrangement of the six paralogous proteasomal AAA+ ATPase subunits in yeast (Figure 7A). The subunits form a heterohexameric ring with a unique arrangement. Specific disulfide bonds between Rpt subunits could be induced in active, fully assembled proteasomes. In the experimentally determined arrangement, Rpt3 and Rpt6 are neighbors, congruent with the close functional overlap of Nas6 and Rpn14, the two RP assembly chaperones that bind these respective ATPases. It also brings together the ATPases bound by the assembly factors Nas2 and Hsm3, which overlap significantly in their assembly roles as well. Consistent with this, we detected a previously unknown chaperone-associated intermediate containing both Rpt3-Rpt6 and Rpt4-Rpt5 but no subunits of the Hsm3 assembly module. The definitive demonstration of both the arrangement of the eukaryotic proteasomal ATPases and the close similarity of their structural interactions to those in the prokaryotic PAN/ARC homohexamers has significant implications for RP structure and mechanism.

Eukaryotic ATPases Form a Specifically Ordered Ring

At present there are no atomic-resolution structures available for the RP or RP base. The six ATPases of eukaryotic proteasomes are found in complexes that usually contain other subunits, including the two largest subunits, Rpn1 and Rpn2. Due to this, it has not yet been possible to demonstrate formally that the six ATPases form a ring. Symmetry analysis of the RP in electron-microscopic reconstructions suggested 6-fold symmetry for densities near the CP in purified 26S proteasomes (Forster et al., 2009), but density assignments to specific ATPase subunits were not determined experimentally. Our crosslinking

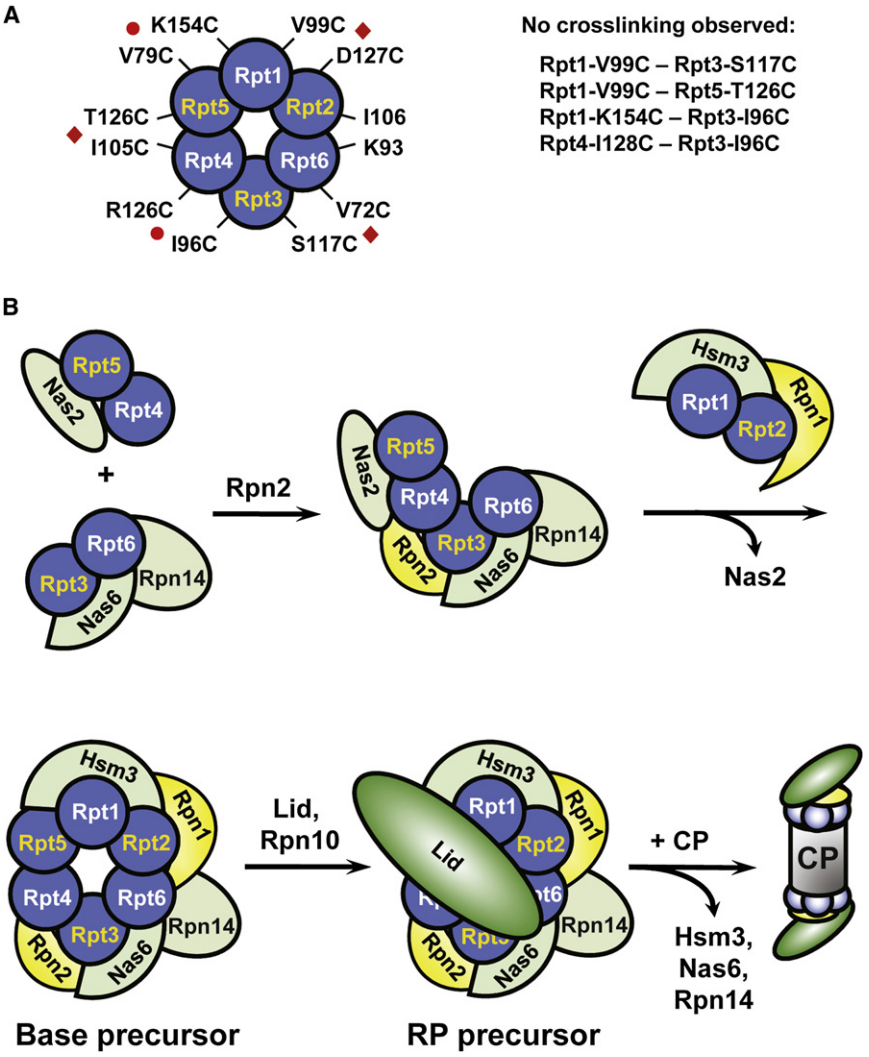

Figure 7. ATPase Arrangement and Revised Model of RP Base Assembly

(A) Arrangement of eukaryotic ATPases based on disulfide crosslinking of the yeast proteasome. Red diamonds indicate engineered disulfides that were observed experimentally within *cis-trans* dimers, and red circles mark interdimer crosslinks.

(B) Updated model of proteasomal RP assembly. The current work suggests a potential assembly intermediate with two ATPase assembly modules that can form without the Hsm3 module. Other two-module intermediates might also be able to form. The joining of Nas6/Rpt3 and Rpn14/Rpt6 into a single module is based on data from mammalian cells (Kaneko et al., 2009).

analysis was based explicitly on the assumption of close similarity—within a few angstroms—between ATPase interactions in the eukaryotic RP compared to those in the ring-shaped PAN homohexamer. Therefore, the highly specific disulfide linkages that were induced between the yeast ATPases provide formal confirmation of the ring arrangement of eukaryotic Rpt subunits suggested by EM analyses.

Although a ring arrangement for the Rpt subunits had been highly probable, it was less certain that the subunits assumed a unique order within such a ring. On the one hand, the similar relative levels of all six ATPases in purified proteasomes (Nickell et al., 2009) was consistent with a single copy of each paralog. On the other, protein-protein interaction data included a number of inconsistencies in ATPase subunit positions. Moreover, none of the previously available data ruled out the possibility of alternative subunit arrangements in different particles that averaged out to a ratio of roughly one copy of each Rpt per RP complex. The arrangement with the fewest discrepancies with published subunit-subunit interaction data matches the arrangement we determined experimentally (Figure 7A) and was the basis for predicting this arrangement in a recent report (Nickell et al., 2009). Our results do not rule out formation of alternative ring arrangements under certain circumstances, but they do argue that the observed order characterizes the great majority of proteasomes under standard growth conditions.

We note that the structure-guided disulfide-engineering approach described here is general and could be used in other systems where homologous but compositionally simpler multisubunit structures are known at atomic resolution. For example, the eukaryotic CCT/TRiC class II chaperonin consists of eight different subunits arrayed in a pair of back-to-back octameric rings; a model for subunit placements has been generated based on subunit associations seen in minicomplexes and antibody-CCT complexes analyzed by EM (Martin-Benito et al., 2007). The crystal structures of the simpler archaeal class II chaperonin (Shomura et al., 2004) could be used to guide disulfide engineering of the eukaryotic complex to test the model. Furthermore, the homology-guided disulfide engineering method can also be used to evaluate potential assembly intermediates, as we have done (Figure 6C).

Organization of the RP Base

As mentioned, Pro91 and its preceding residue in the *M. jannaschii* PAN subunits alternates between the *cis* and *trans* peptide configuration in the homohexamer, allowing N-terminal helices of neighboring subunits to form CCs and create a trimer-of-dimers arrangement. Whether a prolyl isomerase is needed to switch Pro91 or the equivalent Pro residues in the eukaryotic "*cis*" ATPases into the *cis* conformation is an interesting question for future work. Although the sequence alignments by Zhang et al. (2009) suggested that only Rpt2, Rpt3, and Rpt5 among the human and yeast proteasomal ATPases had a Pro residue

corresponding to PAN Pro91, our sequence alignments and those of Djuranovic et al. (2009) indicate that Rpt1 also has a Pro at this position. The engineered Rpt1-Rpt2 disulfide (Figure 3) supports the latter alignments. Rpt1 orthologs in the majority of species share this proline. This raises the possibility that Rpt1 might reorient its N-terminal helix, perhaps to form a CC with another protein separately from Rpt2. A number of non-ATPase subunits in the RP lid and base, such as Rpn1 and Rpn2, have predicted CC sequences.

In the PAN subcomplex I crystal structure (Protein Data Bank [PDB] 3H43), the *cis* and *trans* subunits in each dimer bury a large surface area (2144 $Å^2$), indicating that these associations are quite stable. In contrast, the interdimer interfaces, which lack the CC, bury only 923 $Å^2$ of protein surface (Lee and Richards, 1971), suggesting that proper positioning of Rpt *cis-trans* heterodimers in the ring might require a chaperone-like activity. The RP base chaperones could function in these assembly steps in eukaryotes, which have greater complexity in ATPase ring composition. Alternatively, or in addition, the CP might act as a scaffold or template in RP base assembly. We previously suggested this possibility in light of the RP base assembly defects seen in CP and CP assembly mutants (Kusmierczyk et al., 2008). This hypothesis has recently been extended by Park et al. (2009), who reported evidence suggesting that surface pockets in the outer ring of the CP bind to the C termini of specific ATPases to guide base formation. Recent data also suggest that RP assembly steps can occur on a CP scaffold in human cells (Hendil et al., 2009).

The current results are important for the evaluation of another issue regarding RP structure that has recently been raised, namely the positioning of the two largest subunits, Rpn1 and Rpn2. Modeling and structural studies suggested that the α-solenoid repeats comprising much of Rpn1 and Rpn2 close into toroids that stack directly over the pore in the CP (Rosenzweig et al., 2008; Effantin et al., 2009). The stacked toroids were proposed to fit within the ATPase ring and protrude axially from it. Our results demonstrate that the eukaryotic ATPase subunits form a ring via their CC-OB domains that is extremely similar to the prokaryotic PAN/ARC rings. The central pore observed in the latter structures is only 11–13 Å across, far too small to accommodate a central Rpn1-Rpn2 cylinder. We suggest instead that such Rpn1-Rpn2 structures might form on the CP to create a particle that is functionally distinct from RP2CP, or they may play a role in proteasome assembly. Precisely where the non-ATPase subunits of the RP base are located remains to be determined. EM analyses of 26S proteasomes have suggested several extended electron-dense segments in the periphery of the base region that might accommodate Rpn1 and/or Rpn2 (da Fonseca and Morris, 2008; Nickell et al., 2009). By removing Rpn1 and Rpn2 from the center of the ATPase ring and showing that the eukaryotic ATPases must form a narrow central channel like the homohexameric PAN/ARC proteins, our results suggest that these ATPase complexes all use a common mechanism for unfolding substrates and translocating them into the CP. Key features include the rigid OB domain ring that may provide an anchor for exerting unfolding forces on the substrate and the "Ar-Φ loops" that are thought to help pull the substrate into the CP pore (Wang et al., 2001; Zhang et al., 2009).

Implications for Proteasome Assembly

The experimentally determined arrangement of eukaryotic proteasomal ATPases (Figure 7A) rationalizes some previously puzzling genetic data on the functional overlap of the ATPase-binding RP assembly chaperones (Funakoshi et al., 2009; Saeki et al., 2009). The Nas6 and Rpn14 chaperones display significant redundancy in their functions, as do the other two RP chaperones, Nas2 and Hsm3. However, a previous model for ATPase organization (Figure 1A, model 1) placed the subunits to which these chaperones bind on opposite sides of the ring. With the revised model, the functional overlaps of these two pairs of chaperones are easier to understand (Figure 7B). By binding neighboring ATPases or pairs of ATPases, the chaperones are in position to facilitate assembly of subunits that are in direct contact with one another. From the data in Figure 6, for example, we suggest that Nas2 and Hsm3 help complete ATPase ring assembly by bringing together the Hsm3 assembly module and a complex including the Nas2 and Nas6/Rpn14 assembly modules (and Rpn2). Nas2 is not seen stably associated with any Hsm3-containing complex and may be released either at or close to this joining step. The data do not rule out other higher-order intermediates, such as one involving the Nas6/Rpn14 and Hsm3 modules (Kaneko et al., 2009).

Stepwise assembly of the ATPase ring will help ensure formation of the correct subunit arrangement. Once assembled, incorrect hexamers might not be readily disassembled because of the accumulated buried surfaces of the six subunits. Because energetic differences between incorrect and correct assemblies based on the six OB domain interfaces are minimal, a stochastic collision mechanism for assembly would be error prone. By going through a pathway involving preassembly of specific Rpt heterodimers, many incorrectly assembled rings, such as homohexamers, can be avoided. Some of the *trans* Rpt subunits lack the critical Pro residue needed for them to adopt a *cis* conformation, which should impede their ability to form incorrect dimers. Finally, all the Rpt heterodimers are part of larger subassemblies that include assembly chaperones. These chaperones may present steric barriers that also limit formation of aberrant ring structures.

EXPERIMENTAL PROCEDURES

Yeast and Bacterial Strains

All yeast manipulations were carried out according to standard protocols (Guthrie and Fink, 2002). Yeast strains used in this study are listed in Table S1. To test pairwise interactions between ATPase subunits, we created a set of strains with chromosomal *HIS3*-marked deletions of each *RPT* gene (Rubin et al., 1998) covered by a *URA3*-marked plasmid bearing the corresponding WT *RPT* allele. Singly mutant strains were crossed, and the resulting diploids were subjected to tetrad dissection. Double mutant segregants from four-spore tetrads were identified by colony PCR and/or test crosses to WT cells. Mutant or WT *RPT* alleles carried on *LEU2*- and *TRP1*-marked plasmids were introduced into the appropriate double mutants, and the original *URA3* plasmids were evicted by selection on 5-fluoroorotic acid plates. Epitope tagging of chromosomal loci was done using homologous recombination with PCR fragments amplified from the appropriate template plasmids (Funakoshi and Hochstrasser, 2009).

E. coli strain MC1061 was used for plasmid construction and mutagenesis. Standard methods were used for DNA manipulation, and QuikChange

(Stratagene) was used for site-directed mutagenesis. Mutated alleles were sequenced by automated DNA sequencing (Yale Science Hill core facility).

Disulfide Crosslinking of Engineered Rpt Subunits

Crosslinking of Rpt subunits was performed largely as described for CP analysis (Velichutina et al., 2004) but with some modifications. Briefly, 10–15 OD_{600} equivalents of mid-log phase yeast cells expressing Rpt proteins with the desired cysteine substitutions were converted to spheroplasts, and the spheroplasts were lysed in 0.12 ml of ice-cold lysis buffer (50 mM HEPES [pH 7.5], 150 mM NaCl, 5 mM $MgCl_2$) containing an EDTA-free protease inhibitor cocktail (Roche). Lysis was achieved by vortexing three times at top speed for 30 s intervals with 1 min on ice in between. Cell debris was removed by a 15 min centrifugation at 13,000 × g at 4°C, and 20 μl of supernatant was removed and added to 2 μl of 10× stop buffer (10 mM sodium iodoacetate and 50 mM *N*-ethylmaleimide). Disulfide crosslinking of the remaining extract was induced with 0.2–0.5 mM $CuCl_2$ at room temperature. Aliquots were removed at different times and added to tubes on ice that contained 10× stop buffer. For crosslinking Nas2-FLAG eluates, ~300 OD_{600} equivalents of yeast cells were lysed as above, except the lysis buffer was supplemented with 2 mM ATP. The immunoprecipitations were done as described in the next section.

Immunoblot and Immunoprecipitation Analyses

SDS-PAGE and immunoblot analysis of proteins were carried out according to standard procedures (Li et al., 2007). For immunoblotting, gel-separated protein samples were electrotransferred to PVDF membranes (Millipore). Membranes were incubated with monoclonal or polyclonal antibodies to Rpt1, Rpt4, or Rpn1 (gifts from W. Tansey); Rpt2, Rpt3, or Rpt5 (Enzo Life Sciences); Rpt6 (gift from C. Mann); or base assembly chaperones Nas2, Nas6, Rpn14, or Hsm3 (Funakoshi et al., 2009). Proteins were visualized with ECL (GE Healthcare).

For immunoprecipitation analyses, yeast cell extracts were prepared under nondenaturing conditions essentially as described (Li et al., 2007). Briefly, mid-to-late log phase cells (OD_{600} 1–2) were washed with ice-cold water and frozen in liquid nitrogen. The frozen cells were ground with mortar and pestle, and the resultant cell powder was thawed in buffer A (50 mM Tris-HCl [pH 7.5], 5 mM $MgCl_2$, 10% glycerol, 2 mM ATP, 150 mM NaCl). Extracts were centrifuged for 10 min at 15,000 × g to remove cell debris. After determining protein concentrations (Bio-Rad Protein Assay), normalized samples were incubated with 50 μl FLAG-M2 agarose (Sigma) for 2 hr at 4°C, washed three times with ice-cold buffer A, and bound proteins eluted with 200 μg/ml 3xFLAG peptide (Sigma) for 30 min at 4°C. Eluates were analyzed by immunoblotting as described above.

Analysis of Rpt Associations in Active 26S Proteasomes

To analyze disulfide crosslinked Rpt proteins after native PAGE followed by nonreducing SDS-PAGE, yeast cell extracts were prepared as described above for the immunoprecipitation studies. After determining proteins concentrations, normalized samples were used for native PAGE followed by fluorogenic substrate (Suc-LLVY-AMC; Sigma) overlay and UV light exposure to visualize active proteasomes; the gel was subjected to oxidative crosslinking by incubating in 0.2 mM $CuCl_2$. A gel strip containing the RP2CP bands was excised and placed on a nonreducing SDS gel (Kusmierczyk et al., 2008). Following electrophoresis, proteins were analyzed by immunoblotting.

SUPPLEMENTAL INFORMATION

Supplemental Information includes one table and three figures and can be found with this article online at doi:10.1016/j.molcel.2010.02.035.

ACKNOWLEDGMENTS

This work was supported by a National Institutes of Health (NIH) grant (R01 GM083050 to M.H.). R.J.T. was supported in part by a Brown-Coxe Postdoctoral Fellowship. We thank J. Roelofs and D. Finley for yeast strains, W. Tansey and C. Mann for antibodies to specific Rpt subunits, and M. Kunjappu and A. Kusmierczyk for comments on the manuscript.

Received: December 23, 2009
Revised: February 1, 2010
Accepted: February 16, 2010
Published: May 13, 2010

REFERENCES

Arendt, C.S., and Hochstrasser, M. (1997). Identification of the yeast 20S proteasome catalytic centers and subunit interactions required for active-site formation. Proc. Natl. Acad. Sci. USA *94*, 7156–7161.

Besche, H.C., Peth, A., and Goldberg, A.L. (2009). Getting to first base in proteasome assembly. Cell *138*, 25–28.

Chen, P., and Hochstrasser, M. (1996). Autocatalytic subunit processing couples active site formation in the 20S proteasome to completion of assembly. Cell *86*, 961–972.

da Fonseca, P.C., and Morris, E.P. (2008). Structure of the human 26S proteasome: subunit radial displacements open the gate into the proteolytic core. J. Biol. Chem. *283*, 23305–23314.

Djuranovic, S., Hartmann, M.D., Habeck, M., Ursinus, A., Zwickl, P., Martin, J., Lupas, A.N., and Zeth, K. (2009). Structure and activity of the N-terminal substrate recognition domains in proteasomal ATPases. Mol. Cell *34*, 580–590.

Effantin, G., Rosenzweig, R., Glickman, M.H., and Steven, A.C. (2009). Electron microscopic evidence in support of alpha-solenoid models of proteasomal subunits Rpn1 and Rpn2. J. Mol. Biol. *386*, 1204–1211.

Finley, D. (2009). Recognition and processing of ubiquitin-protein conjugates by the proteasome. Annu. Rev. Biochem. *78*, 477–513.

Forster, F., Lasker, K., Beck, F., Nickell, S., Sali, A., and Baumeister, W. (2009). An atomic model AAA-ATPase/20S core particle sub-complex of the 26S proteasome. Biochem. Biophys. Res. Commun. *388*, 228–233.

Fu, H., Reis, N., Lee, Y., Glickman, M.H., and Vierstra, R.D. (2001). Subunit interaction maps for the regulatory particle of the 26S proteasome and the COP9 signalosome. EMBO J. *20*, 7096–7107.

Funakoshi, M., and Hochstrasser, M. (2009). Small epitope-linker modules for PCR-based C-terminal tagging in Saccharomyces cerevisiae. Yeast *26*, 185–192.

Funakoshi, M., Tomko, R.J., Jr., Kobayashi, H., and Hochstrasser, M. (2009). Multiple assembly chaperones govern biogenesis of the proteasome regulatory particle base. Cell *137*, 887–899.

Guthrie, C., and Fink, G.R. (2002). Guide to Yeast Genetics and Molecular and Cell Biology, Volumes 350 and 351 (San Diego: Academic Press).

Hartmann-Petersen, R., Tanaka, K., and Hendil, K.B. (2001). Quaternary structure of the ATPase complex of human 26S proteasomes determined by chemical cross-linking. Arch. Biochem. Biophys. *386*, 89–94.

Hendil, K.B., Kriegenburg, F., Tanaka, K., Murata, S., Lauridsen, A.M., Johnsen, A.H., and Hartmann-Petersen, R. (2009). The 20S proteasome as an assembly platform for the 19S regulatory complex. J. Mol. Biol. *394*, 320–328.

Kaneko, T., Hamazaki, J., Iemura, S., Sasaki, K., Furuyama, K., Natsume, T., Tanaka, K., and Murata, S. (2009). Assembly pathway of the mammalian proteasome base subcomplex is mediated by multiple specific chaperones. Cell *137*, 914–925.

Kusmierczyk, A.R., Kunjappu, M.J., Funakoshi, M., and Hochstrasser, M. (2008). A multimeric assembly factor controls the formation of alternative 20S proteasomes. Nat. Struct. Mol. Biol. *15*, 237–244.

Le Tallec, B., Barrault, M.B., Guerois, R., Carre, T., and Peyroche, A. (2009). Hsm3/S5b participates in the assembly pathway of the 19S regulatory particle of the proteasome. Mol. Cell *33*, 389–399.

Lee, B., and Richards, F.M. (1971). The interpretation of protein structures: estimation of static accessibility. J. Mol. Biol. *55*, 379–400.

Li, X., Kusmierczyk, A.R., Wong, P., Emili, A., and Hochstrasser, M. (2007). beta-Subunit appendages promote 20S proteasome assembly by overcoming an Ump1-dependent checkpoint. EMBO J. *26*, 2339–2349.

Marques, A.J., Palanimurugan, R., Matias, A.C., Ramos, P.C., and Dohmen, R.J. (2009). Catalytic mechanism and assembly of the proteasome. Chem. Rev. *109*, 1509–1536.

Martin-Benito, J., Grantham, J., Boskovic, J., Brackley, K.I., Carrascosa, J.L., Willison, K.R., and Valpuesta, J.M. (2007). The inter-ring arrangement of the cytosolic chaperonin CCT. EMBO Rep. *8*, 252–257.

Nickell, S., Beck, F., Scheres, S.H., Korinek, A., Forster, F., Lasker, K., Mihalache, O., Sun, N., Nagy, I., Sali, A., et al. (2009). Insights into the molecular architecture of the 26S proteasome. Proc. Natl. Acad. Sci. USA *106*, 11943–11947.

Park, S., Roelofs, J., Kim, W., Robert, J., Schmidt, M., Gygi, S.P., and Finley, D. (2009). Hexameric assembly of the proteasomal ATPases is templated through their C termini. Nature *459*, 866–870.

Ravid, T., and Hochstrasser, M. (2008). Diversity of degradation signals in the ubiquitin-proteasome system. Nat. Rev. Mol. Cell Biol. *9*, 679–690.

Rosenzweig, R., Osmulski, P.A., Gaczynska, M., and Glickman, M.H. (2008). The central unit within the 19S regulatory particle of the proteasome. Nat. Struct. Mol. Biol. *15*, 573–580.

Rubin, D.M., Glickman, M.H., Larsen, C.N., Dhruvakumar, S., and Finley, D. (1998). Active site mutants in the six regulatory particle ATPases reveal multiple roles for ATP in the proteasome. EMBO J. *17*, 4909–4919.

Saeki, Y., Toh, E.A., Kudo, T., Kawamura, H., and Tanaka, K. (2009). Multiple proteasome-interacting proteins assist the assembly of the yeast 19S regulatory particle. Cell *137*, 900–913.

Shomura, Y., Yoshida, T., Iizuka, R., Maruyama, T., Yohda, M., and Miki, K. (2004). Crystal structures of the group II chaperonin from Thermococcus strain KS-1: steric hindrance by the substituted amino acid, and inter-subunit rearrangement between two crystal forms. J. Mol. Biol. *335*, 1265–1278.

Thompson, D., Hakala, K., and DeMartino, G.N. (2009). Subcomplexes of PA700, the 19 S regulator of the 26 S proteasome, reveal relative roles of AAA subunits in 26 S proteasome assembly and activation and ATPase activity. J. Biol. Chem. *284*, 24891–24903.

Velichutina, I., Connerly, P.L., Arendt, C.S., Li, X., and Hochstrasser, M. (2004). Plasticity in eucaryotic 20S proteasome ring assembly revealed by a subunit deletion in yeast. EMBO J. *23*, 500–510.

Wang, J., Song, J.J., Franklin, M.C., Kamtekar, S., Im, Y.J., Rho, S.H., Seong, I.S., Lee, C.S., Chung, C.H., and Eom, S.H. (2001). Crystal structures of the HslVU peptidase-ATPase complex reveal an ATP-dependent proteolysis mechanism. Structure *9*, 177–184.

Zhang, F., Hu, M., Tian, G., Zhang, P., Finley, D., Jeffrey, P.D., and Shi, Y. (2009). Structural insights into the regulatory particle of the proteasome from Methanocaldococcus jannaschii. Mol. Cell *34*, 473–484.